

Subpicosecond molecular dynamics studied by degenerate four-wave mixing with incoherent light

Kenji Kurokawa, Toshiaki Hattori, and Takayoshi Kobayashi

Department of Physics, Faculty of Science, University of Tokyo, 7-3-1 Hongo, Bunkyo-ku, Tokyo 113, Japan

(Received 20 March 1987)

A time-resolved study of the relaxation times of the third-order susceptibility for the optical Kerr effect in CS₂ and nitrobenzene was made by degenerate four-wave mixing using 5-ns pulses from a broadband laser. In the case of CS₂ we observed both subpicosecond (~ 0.2 ps) and picosecond (~ 2 ps) relaxation times for the susceptibility tensor element of $\chi_{xyyx}^{(3)}$ and $\chi_{xxxx}^{(3)}$ both at 553 and 623 nm. The observed relaxation times agree with those obtained utilizing subpicosecond pulses. The relaxation times of nitrobenzene could not be measured because the shorter relaxation time is shorter than the resolution time and the longer one is longer than that of CS₂.

I. INTRODUCTION

Liquid CS₂ is one of the most familiar optical Kerr media with a large nonlinear refractive index n_2 .¹ In 1975, a direct time-resolved measurement using a picosecond laser revealed that the relaxation time of optically induced birefringence in CS₂ is 2.1 ps.² The recent development of the generation technique of subpicosecond and femtosecond optical pulses made easier the relaxation-time measurement of the optical Kerr effect with higher time resolution. Using a time-resolved interferometric technique with 70-fs pulses at 619.5 nm, Halbout and Tang observed both a 2.00- and 0.33-ps response with standard deviations comparable to the experimental resolution time (~ 17 fs).³ Greene and Farrow measured two relaxation times, 2.16 ± 0.1 and 0.24 ± 0.02 ps, utilizing a biased Kerr shutter with 150-fs pulses at 620 nm.⁴ Using a usual Kerr shutter with 200-fs pulses, Etchepare *et al.* observed a response of 1.4 ± 0.1 and 0.20 ± 0.05 ps. Pulses with two wavelengths were used in their measurement, 615 nm for the pump pulse and 650 nm for the probe pulse.⁵ In all three measurements subpicosecond (0.2–0.3 ps) and picosecond (1.4–2.2 ps) relaxations with almost the same corresponding time constants were observed. Also in the frequency domain, Trebino *et al.* measured the relaxation times of four nonzero third-order susceptibility elements for the optical Kerr effect in CS₂ using a tunable-laser-induced-grating technique with an excitation wavelength of 575 nm and a probe wavelength of 570 nm. They obtained, for example, two relaxation times of 2.49 ± 0.5 and 0.21 ± 0.04 ps for $\chi_{xxxx}^{(3)}$.⁶

The picosecond relaxation in CS₂ is considered to be associated with orientational randomization by rotational diffusion of molecules. On the other hand, the mechanism of the subpicosecond response is not well explained. Several mechanisms have been proposed as its possible physical origin: the damped-librational motion, the time-dependent behavior resulting from collisions, and the short-time behavior associated with the rotational diffusion of molecules possessing a large anisotropic polarizability.^{3,4,6,7}

Liquid nitrobenzene is also one of the well-known optical Kerr media. Tang and Halbout observed a subpicosecond relaxation time (~ 150 fs) with an inter-

ferometric technique.³ Etchepare *et al.* observed subpicosecond (< 0.2 ps) and picosecond (4 and 42 ps) relaxation times with a Kerr shutter.⁵

The development of the generation technique of subpicosecond and femtosecond pulses made possible the direct observation of ultrafast phenomena. However, there are several difficulties such as the limited wavelength range of these short pulses and the broadening of the pulse duration in dispersive media. Recently a new spectroscopic technique, coherent-transient spectroscopy with incoherent light, has been presented both theoretically and experimentally.^{8–21} It was suggested theoretically that the time resolution of the degenerate four-wave mixing (DFWM) in the measurement of the transverse relaxation time (T_2) is not limited by the pulse duration but determined only by the correlation time of the excitation light, which can be much shorter than the pulse duration. Theoretical correlation profiles were calculated for various ratios of T_2 and T_1 (the longitudinal relaxation time) by a perturbational method.⁹ Via photon echoes the transverse relaxation times of several systems were measured using an incompletely mode-locked synchronously pumped dye laser or a nanosecond dye laser pumped by a nitrogen laser.^{8,10,12,21} The longitudinal relaxation time (T_1) was also measured with the time resolution limited only by the intensity correlation time of the excitation pulse.¹⁹ Recently it was proposed and demonstrated that the vibrational dephasing time can also be measured by coherent Stokes Raman scattering using both coherent and incoherent light with the time resolution determined by the correlation time of the incoherent light.²⁰

In this paper the authors report for the first time the time-resolved optical phase conjugation in Kerr liquids, CS₂ and nitrobenzene, using incoherent light. The subpicosecond (~ 0.2 ps) and the picosecond (~ 2 ps) relaxation times were observed in CS₂. The details of the experimental procedure and results obtained by the time-resolved phase conjugation in CS₂ and nitrobenzene are presented in the following sections.

II. EXPERIMENTAL PROCEDURE

The experimental setup used for the measurements of the phase-conjugate signal in both Kerr liquids is shown

in Fig. 1. The light source was a dye laser pumped by an excimer laser (Hamamatsu C2540). The dye laser is constituted of an oscillator and a single-stage amplifier. To obtain incoherent light, the oscillator cavity with no tuning element was constructed by inserting an end mirror between the dye cell and the beam expander in a commercial dye laser cavity (Molelectron DL-14). The spectrum of the dye laser light was measured by a system consisting of a polychromator and a multichannel photodiode array detector (MCPD) which was controlled by a microcomputer. Rhodamine 560 (Rh 560) in methanol or Rhodamine 640 (Rh 640) in ethanol was used as the laser dye both in the oscillator and the amplifier. The center wavelength was 553 nm and the width [full width at half maximum (FWHM)] of the spectrum was 5.5 nm for Rh 560, and these values for Rh 640 were 623 and 5.0 nm.

The dye laser beam was passed through a Rochon prism to obtain a linearly polarized beam. The linearly polarized beam was split into three beams I_1 , I_2 , and I_3 by beam splitters BS1 and BS2. After passing through delay lines, beams I_3 and I_2 were focused in the sample by lenses L1 ($f=70$ mm) and L2 ($f=100$ mm), respectively. Lengths of the delay lines were varied with stepping motors. In all measurements beam I_2 was delayed or advanced by 0.2 ns to the other two beams, I_1 and I_3 , and had no correlation with them because the correlation time of the dye laser light was in subpicosecond region. The signal intensity was measured as a function of the delay time (τ) of beam I_1 with respect to beam I_3 . Beam I_1 was made parallel to beam I_3 and was focused in the sample by lens L1. Beams I_1 and I_2 were exactly counterpropagating to each other. The duration of the pulses was 5 ns. The peak intensities of beams I_1 , I_2 , and I_3 in the focal plane when Rh 560 was used as the laser dye were about 200, 400, and 300 MW/cm², respectively. These values for Rh 640 were about 70, 200, and 100 MW/cm², respectively. Polarization planes of the three beams can be independently changed with three half-wave retarders, each of which is composed of coupled Fresnel rhombs. Measurements were performed in two types of polarization configurations. The two types are denoted as follows:

Type I: I_1 and I_2 are horizontally polarized and I_3 is vertically polarized.

Type II: I_1 , I_2 , and I_3 are all vertically polarized.

The sample was in a 1-cm cell. The angle between beams I_1 and I_3 was 4° in the sample cell. The phase-conjugate signal was split by a glass plate BS3 and detected with a photodiode after passing through an analyzer polarizer (PL). Output intensity of the photodiode coupled with a sample-and-hold circuit was digitized and transferred to a microcomputer. The excimer laser and all the circuits for detection were synchronized and controlled by a synchronizing circuit and the microcomputer.

III. RESULTS AND DISCUSSION

The semilogarithmic intensity of the normalized phase-conjugate signal in CS₂ obtained with 553-nm laser is shown in Fig. 2. Beam I_2 was delayed by about 0.2 ns with respect to the other two beams. The polarization configuration was type I, that is, I_1 and I_2 were horizontally polarized and I_3 was vertically polarized. Figure 2 also shows a semilogarithmic plot of the normalized signal in a reference sample, which is a solution of 4-diethylamino-4'-nitrostilbene (DEANS) in CS₂ with a concentration of 1×10^{-3} mole/l. The absorbance of the reference sample was 0.08 at 553 nm. In the measurement with the reference sample the polarization

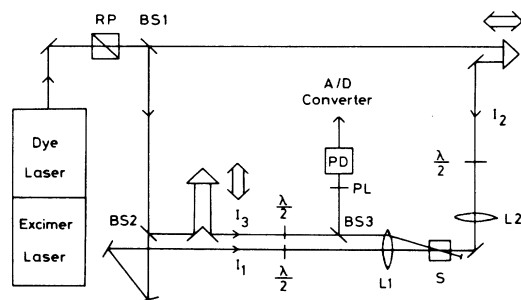


FIG. 1. Experimental setup for the degenerate four-wave mixing using incoherent light. BS1 and BS2 are the beam splitters; BS3, the glass plate; L1, L2, the lens; PD, the photodiode; PL, the polarizer; RP, the Rochon prism; S, the sample; $\lambda/2$, the half-wave retarder.

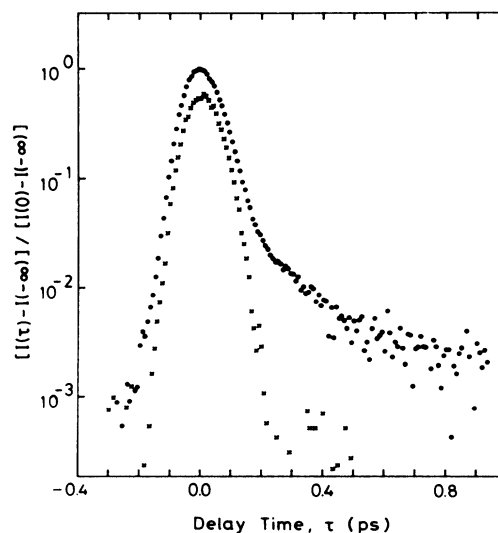


FIG. 2. Normalized signal intensity as a function of delay time τ of I_1 to I_3 . Signal intensity is normalized by the difference between the intensity at $\tau=0, I_s(0)$, and the intensity at $\tau=-\infty, I_s(-\infty)$. (●), CS₂ in type-I polarization configuration, where I_3 is vertically polarized and both I_1 and I_2 are horizontally polarized. (×), reference sample (DEANS) in CS₂ in type-II polarization configuration, where I_1 , I_2 , and I_3 are all vertically polarized. The wavelength is 553 nm. Plot of the normalized signal intensity in reference sample is slightly shifted down.

configuration was type II, that is, all three beams were vertically polarized. Since the signal intensity in the reference sample is mainly due to the thermal grating, and it is more than two orders of magnitude larger than that in neat CS₂, the effect of the signal due to the nonlinearity of CS₂ itself is negligible. As shown in Fig. 2 the signal obtained for the reference sample is symmetric with respect to the delay time and its FWHM is 0.12 ps. Since I_2 has no correlation with the other two, the observed signal in the reference sample is considered to be due to a thermal grating produced by the interference between beams I_1 and I_3 . The observed signal, therefore, gives a correlation profile $|G(\tau)|^2$ of the incident incoherent light, where $G(\tau)$ is the autocorrelation of the incoherent field

$$G(\tau) = \langle E^*(t)E(t+\tau) \rangle. \quad (1)$$

On the other hand, the signal in CS₂ is clearly asymmetric and consists of three components with different decay times. The signal shape was independent of the scan direction of the delay time. The time dependence of the signal in the case when the beam I_2 was advanced by about 0.2 ns to the other two was the same as in Fig. 2. In Fig. 2 the fastest decay component among the three is very intense and its time dependence coincides with the reference signal, that is, with the correlation profile $|G(\tau)|^2$. In order to determine the longest decay time, measurement in a wider delay-time range was performed, the result being shown in Fig. 3. The time constant τ_l was obtained as 0.9 ± 0.1 ps. By subtracting the slowest component, the time constant τ_s of the middle component was obtained as 88 ± 8 fs. Twice these obtained values, that is, $2\tau_l = 1.8 \pm 0.4$ ps and $2\tau_s = 0.18 \pm 0.02$ ps, agree within experimental error with the long and short time constants, respectively, obtained by ultrashort pulses or by the frequency-domain measurements as mentioned in Sec. I.

Figure 4 shows a semilogarithmic plot of the DFWM signal intensity in CS₂ measured in the type-II polariza-

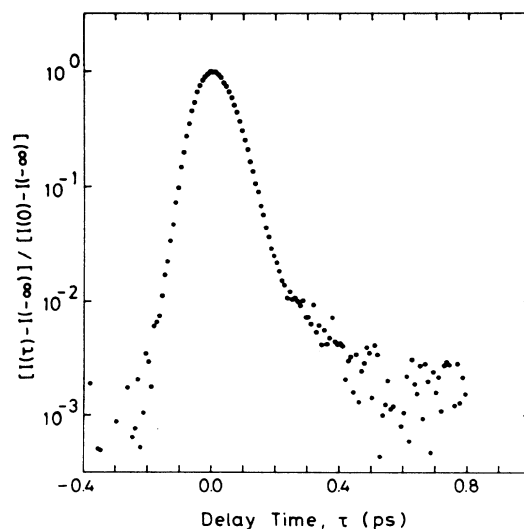


FIG. 4. Normalized signal intensity as a function of delay time in CS₂ at 553 nm. Polarization configuration is type II.

tion configuration at 553 nm. The signal profile is almost the same as in Fig. 2 and is composed of three components. The determination of the time constant τ_l is difficult because of the small signal-to-noise ratio. The obtained value of τ_s is 100 ± 30 fs and is in agreement with the data of the type I polarization configuration.

Figure 5 shows a semilogarithmic plot of the signal intensity in CS₂ of type-I polarization configuration at 623 nm. The time constants τ_l and τ_s were obtained as 0.8 ± 0.4 ps and 100 ± 15 fs, respectively. These values agree within experimental errors with those at 553 nm. Two time constants τ_l and τ_s of type-II polarization configuration were also obtained at 623 nm and agreed

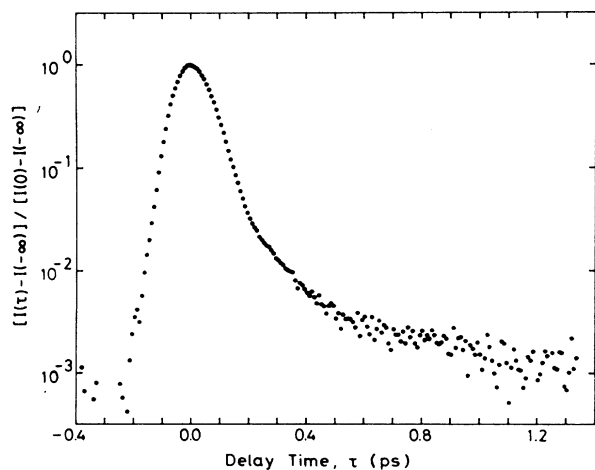


FIG. 3. Normalized signal intensity as a function of delay time in CS₂ at 553 nm. Polarization configuration is type I.

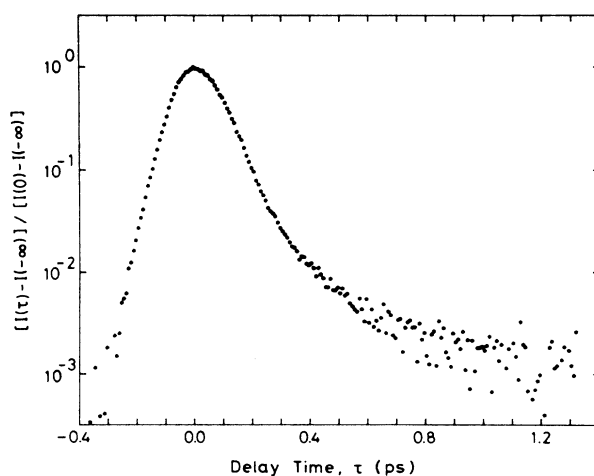


FIG. 5. Normalized signal intensity as a function of delay time in CS₂ at 623 nm. Polarization configuration is type I.

within experimental errors with respective values of the type-I polarization configuration.

According to the theory based on the Born-Oppenheimer approximation,²² the third-order nonlinear polarization $P^{(3)}$ in optically transparent media has the form

$$P_i^{(3)}(t) = \sigma_{ijkl} E_j(t) E_k(t) E_l(t) + E_j(t) \int_{-\infty}^t dt' d_{ijkl}(t-t') E_k(t') E_l(t'), \quad i=x,y,z \quad (2)$$

where σ_{ijkl} is a constant tensor which describes the electronic nonlinearity and $d_{ijkl}(t)$ represents the nuclear contribution to the third-order polarization. $E_i(t)$ denotes i ($=x,y,z$) component of the total electric field in the medium. For the following discussion, the two contributions are put together for convenience as follows:

$$P_i^{(3)}(t) = E_j(t) \int_{-\infty}^t dt' r_{ijkl}(t-t') E_k(t') E_l(t'), \quad (3)$$

with

$$r_{ijkl}(t) = \sigma_{ijkl} \delta(t) + d_{ijkl}(t). \quad (4)$$

The total electric field $E_i(t)$ can be written in the present case as

$$E_i(t, \mathbf{r}) = E_{(1)i}(t) \exp[i(\omega t - \mathbf{k}_1 \cdot \mathbf{r})] + E_{(2)i}(t) \exp[i(\omega t - \mathbf{k}_2 \cdot \mathbf{r})] + E_{(3)i}(t) \exp[i(\omega t - \mathbf{k}_3 \cdot \mathbf{r})] + \text{c.c.}, \quad (5)$$

with

$$\mathbf{k}_1 + \mathbf{k}_2 = \mathbf{0}, \quad (6)$$

where $E_{(\alpha)i}(t)$ is the time-varying amplitude of the electric field corresponding to beam I_α and c.c. stands for complex conjugates of the preceding terms. From Eqs. (3)–(6) the third-order nonlinear polarization generating a phase-conjugate wave is written as

$$P_i^{(3)}(t, \mathbf{r}) = \exp[i(\omega t + \mathbf{k}_3 \cdot \mathbf{r})] \left\{ E_{(2)j}(t) \int_{-\infty}^t dt' r_{ijkl}(t-t') E_{(1)k}(t') E_{(3)l}^*(t') + E_{(1)j}(t) \int_{-\infty}^t dt' r_{ijkl}(t-t') E_{(2)k}(t') E_{(3)l}^*(t') + E_{(3)j}^*(t) \int_{-\infty}^t dt' r_{ijkl}(t-t') \exp[-2i\omega(t-t')] E_{(1)k}(t') E_{(2)l}(t') + (k \rightleftharpoons l) \right\} + \text{c.c.}, \quad (7)$$

where $(k \rightleftharpoons l)$ means the repetition of the first three terms after permutation of k and l subindices of the electric fields. Since the integrands of the third and the corresponding $(k \rightleftharpoons l)$ terms of Eq. (7) oscillate with frequency 2ω , these terms have little contribution to the third-order nonlinear polarization $P_i^{(3)}(t, \mathbf{r})$.

Then in the case of the type-I polarization configuration, that is, I_3 is vertically (x direction) polarized and I_1 and I_2 are horizontally (y direction) polarized, the third-order nonlinear polarization $P_x^{(3)}(t)$ becomes

$$P_x^{(3)}(t) = \exp[i(\omega t + \mathbf{k}_3 \cdot \mathbf{r})] \left\{ E_{(2)y}(t) \int_{-\infty}^t dt' [r_{xyyx}(t-t') E_{(1)y}(t') E_{(3)x}^*(t') + r_{xyxy}(t-t') E_{(3)x}^*(t') E_{(1)y}(t')] + E_{(1)j}(t) \int_{-\infty}^t dt' [r_{xyyx}(t-t') E_{(2)y}(t') E_{(3)x}^*(t') + r_{xyxy}(t-t') E_{(3)x}^*(t') E_{(2)y}(t')] \right\}. \quad (8)$$

In the present experimental condition the field amplitudes can be described as

$$E_{(1)i}(t) = C_{(1)i} A(t), \quad (9)$$

$$E_{(2)i}(t) = C_{(2)i} A(t - \tau'), \quad (10)$$

$$E_{(3)i}(t) = C_{(3)i} A(t + \tau), \quad (11)$$

where $A(t)$ is the complex field amplitude normalized as

$$\int_{-\infty}^{\infty} dt |A(t)|^2 = 1. \quad (12)$$

The electric field of the incoherent light is assumed to be expressed in terms of a stationary complex Gaussian random process.²³ The complex amplitude of the field $A(t)$ then can be expressed as⁹

$$A(t) = \epsilon(t) R(t), \quad (13)$$

where $\epsilon(t)$ is constant in the time range of observation. $R(t)$ is a complex random function representing a stationary complex Gaussian random process for which

$$\langle R^*(t) R(t + \tau) \rangle = f(\tau), \quad (14)$$

$$\langle R(t) R(t + \tau) \rangle = \langle R^*(t) R^*(t + \tau) \rangle = 0, \quad (15)$$

$$\langle R(t) \rangle = \langle R^*(t) \rangle = 0, \quad (16)$$

where the symbol $\langle \rangle$ represents the statistical average over the random variable of the stochastic process, and the autocorrelation function $f(\tau)$ is proportional to the autocorrelation function of the field $G(\tau)$ which is defined by Eq. (1). The autocorrelation function $f(\tau)$ is assumed to be

$$f(\tau) = \exp(-|\tau|/\tau_c). \quad (17)$$

The incoherent light utilized in experiments may not have the characteristic expressed in Eq. (17), but the signal intensity calculated under the assumption is expected to offer a good approximate value in the delay-time region longer than τ_c .

After the introduction of the stochastic process, physical quantities we can detect should be expressed in terms

of statistical averages over the stochastic variables. The statistical average of the phase-conjugate signal intensity $I_s(\tau)$ is written as

$$I_s(\tau) \propto \langle |P_x^{(3)}(t)|^2 \rangle. \quad (18)$$

From Eqs. (8)–(13) and using the relation²² $r_{xyxy} = r_{xyyx}$, we can rewrite this equation as

$$I_s(\tau) \propto (C_{(1)y} C_{(2)y} C_{(3)x})^2 |\epsilon(t-\tau')|^2 |\epsilon(t)|^4 F(\tau), \quad (19)$$

$$F(\tau) = \sum_{i=1}^3 \int_{-\infty}^t dt' \int_{-\infty}^t ds' r_{xyyx}(t-t') \times r_{xyyx}(t-s') M_i(t', s', \tau), \quad (20)$$

$$M_1 = \langle R(t-\tau') R^*(t-\tau') R(t') R^*(t'+\tau) \times R^*(s') R(s'+\tau) \rangle, \quad (21)$$

$$M_2 = \langle R(t) R^*(t) R(t'-\tau') R^*(t'+\tau) \times R^*(s'-\tau') R(s'+\tau) \rangle, \quad (22)$$

$$M_3 = 2 \langle R(t-\tau') R^*(t) R(t') R^*(t'+\tau) \times R^*(s'-\tau') R(s'+\tau) \rangle. \quad (23)$$

Using the property of the moment of stationary complex Gaussian random process,²³ a sixth-order moment can be factorized with second-order moments. Since τ' is far longer than the correlation time of $R(t)$ in the present case, the sixth-order moment can be factorized with two second-order moments, for example,

$$M_1 = \langle R(t-\tau') R^*(t-\tau') \rangle \times [\langle R(t') R^*(t'+\tau) \rangle \langle R^*(s') R(s'+\tau) \rangle + \langle R(t') R^*(s') \rangle \langle R^*(t'+\tau) R(s'+\tau) \rangle]. \quad (24)$$

For the following discussion the relaxation of r_{ijkl} is assumed to be exponential with a decay-time constant T ,

$$r_{xyyx}(t-t') = r_{xyyx}(0) \exp[-(t-t')/T], \quad (25)$$

and the decay-time constant T is assumed to be much larger than the correlation time τ_c ,

$$T \gg \tau_c. \quad (26)$$

Then $F(\tau)$, which gives delay-time dependence of the signal intensity, is obtained as

$$F(\tau) = [r_{xyyx}(0)]^2 [T^2 \exp(-2|\tau|/\tau_c) + B + T\tau_c], \quad (27)$$

with

$$B = \begin{cases} \frac{\tau_c^2}{2} \exp(-2|\tau|/\tau_c), & \tau \leq 0 \\ \frac{3\tau_c^2}{2} \exp(-2\tau/T) - \tau_c(\tau_c + \tau) \exp(-2\tau/\tau_c), & \tau > 0. \end{cases} \quad (28)$$

$$(29)$$

The delay-time dependence of the signal intensity in the type-II polarization configuration can be also obtained from Eqs. (27)–(29) by replacing r_{xyyx} and T with r_{xxxx} and T' , respectively, where T' is the relaxation time of r_{xxxx} . The first term of Eq. (27) forms a spike at $\tau=0$ in $I_s(\tau)$. We denote this term as the “spike” term. The second term of Eq. (27) decays with a time constant of $T/2$ for long delay time $\tau > \tau_c$. Therefore, this term provides direct information on the relaxation time which is much shorter than the pulse duration. We denote this term as the “signal” term. Since this term has a sharp rise near $|\tau| \sim \tau_c$, the time resolution is determined by the correlation time τ_c . The third term in Eq. (27) appears as a background which is independent of the delay time in $I_s(\tau)$. We denote this term as the “background” term. From Eqs. (27)–(29) relative contributions of the spike term, the signal term, and the background term estimated at $\tau=0$ are T^2 , $\tau_c^2/2$, and $T\tau_c$, respectively. Therefore, the first component in the observed signal is considered to be due to the spike term. The effect described by the spike term is the same one known as the coherence effect involved in the time-resolved optical Kerr effect.²⁴

The middle and the slowest decay components in the observed signals shown in Figs. 2–5 are considered to be due to the signal term. In the delay-time range where the delay time τ is much longer than the correlation time τ_c the signal term decays with time constant $T/2$. Thus, from the measured decay-time constants $\tau_1 = 0.9_{-0.1}^{+0.2}$ ps and $\tau_2 = 88 \pm 8$ fs, relaxation times of the third-order non-linear polarization in CS₂ are obtained to be $1.8_{-0.2}^{+0.4}$ and 0.18 ± 0.02 ps. As previously mentioned, these values agree well with the two time constants determined by the measurements using ultrashort optical pulses.

If we assume the third-order nonlinear polarization is purely electronic, that is, $r_{xyyx}(t) = \sigma_{xyyx} \delta(t)$, then $I_s(-\infty)$ becomes one-half of $I_s(0)$ from Eqs. (19)–(23). In the present measurements in the type-I polarization configuration $I_s(-\infty)$ was about 3% of $I_s(0)$. Therefore, the nuclear contribution is considered to play a major role in r_{xyyx} . This result coincides with the previous study using ultrashort pulses.^{4,25}

Figures 6 and 7, respectively, show semilogarithmic plots of the signals in nitrobenzene in the type-I and -II polarization configurations at 553 nm, with the beam I_2 being delayed by about 0.2 ns with respect to the others. The observed signals of type I and II coincide with each other and are symmetric and composed of only one component, and no asymmetric component could be observed. The signal intensity of type II was about thirty times larger than that of type I. The type-II signal is therefore considered to be mainly due to a thermal grating and gives a correlation profile $|G(\tau)|^2$ of the incident incoherent light. Thus, the observed signal of type I is considered to be due to the spike term mentioned above. It is considered that because of the large ratio of $T^2:\tau_c^2$ due to a longer rotational relaxation time in nitrobenzene [4 and 42 ps (Ref. 5)] than that in CS₂, and because of a shorter relaxation time^{3,5} than the correlation time, any asymmetric component corresponding to the signal term could not be observed in nitrobenzene.

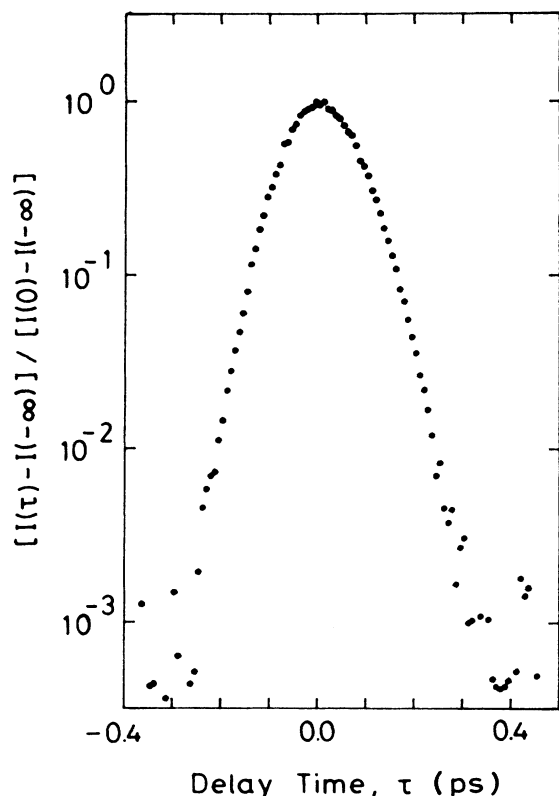


FIG. 6. Normalized signal intensity as a function of delay time in nitrobenzene at 553 nm. The polarization configuration is type I.

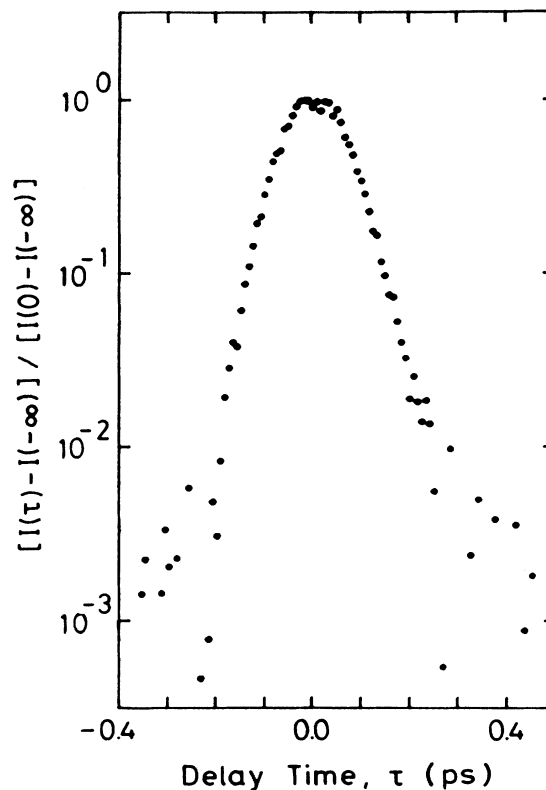


FIG. 7. Normalized signal intensity as a function of delay time in nitrobenzene at 553 nm. The polarization configuration is type II.

In summary, we made a time-resolved study of subpicosecond molecular dynamics in CS_2 and nitrobenzene by the transient degenerate four-wave mixing using incoherent light. The observed signals with CS_2 both at 553 and 623 nm consist of three decay components, two of which are characterized by exponential decays. The fastest decaying component of the three coincides with the correlation profile $|G(\tau)|^2$ of the incident incoherent light. This component is considered as due to the same one as the coherence effect in the time-resolved optical Kerr effect. The middle and slowest decay components provide direct information on the relaxation times in CS_2 . The two relaxation times obtained from these components agree with the two time constants measured by the use of ultrashort optical pulses. In the case of nitrobenzene the

observed signal is symmetric and consists of one component corresponding to the fastest decaying component of the signal observed in CS_2 . It is considered that because of a longer rotational relaxation time than that in CS_2 , and because of a shorter relaxation time than the correlation time of the incoherent light, any asymmetric component which provides direct information on the relaxation time could not be observed in nitrobenzene.

ACKNOWLEDGMENTS

This work is in part supported by a Grant-in-Aid for Special Distinguished Research (56222005) from the Ministry of Education, Science and Culture of Japan.

¹R. Y. Chiao, E. Garmire, and C. H. Townes, *Phys. Rev. Lett.* **13**, 479 (1964).

²E. P. Ippen and C. V. Shank, *Appl. Phys. Lett.* **26**, 92 (1975).

³J. M. Halbout and C. L. Tang, *Appl. Phys. Lett.* **40**, 765 (1982); C. L. Tang and J. M. Halbout, in *Picosecond Phenomena III*, edited by K. B. Eisenthal, R. W. Hochstrasser, W. Kaiser, and A. Laubereau (Springer, Berlin, 1982), p. 212.

⁴B. I. Greene and R. C. Farrow, *J. Chem. Phys.* **77**, 4779 (1982); B. I. Greene and R. C. Farrow, in *Picosecond Phenomena III*,

edited by K. B. Eisenthal, R. W. Hochstrasser, W. Kaiser, and A. Laubereau (Springer, Berlin, 1982), p. 209.

⁵J. Etchepare, G. Grillon, R. Astier, J. L. Martin, C. Bruneau, and A. Antonetti, in *Picosecond Phenomena III*, edited by K. B. Eisenthal, R. M. Hochstrasser, W. Kaiser, and A. Laubereau (Springer, Berlin, 1982), p. 217; J. Etchepare, G. Grillon, and A. Antonetti, *Chem. Phys. Lett.* **107**, 489 (1984).

⁶R. Trebino, C. E. Barker, and A. E. Siegman, *IEEE J. Quantum Electron.* **QE-22**, 1413 (1986).

- ⁷M. Golombok and G. A. Kenney-Wallace, in *Ultrafast Phenomena IV*, edited by D. H. Auston and K. B. Eisenthal (Springer, Berlin, 1984), p. 383.
- ⁸S. Asaka, H. Nakatsuka, N. Fujiwara, and M. Matsuoka, *Phys. Rev. A* **29**, 2286 (1984).
- ⁹N. Morita and T. Yajima, *Phys. Rev. A* **30**, 2525 (1984).
- ¹⁰H. Nakatsuka, M. Tomita, M. Fujiwara, and S. Asaka, *Opt. Commun.* **52**, 150 (1984).
- ¹¹R. Beach and S. R. Hartmann, *Phys. Rev. Lett.* **53**, 663 (1984).
- ¹²M. Fujiwara, R. Kuroda, and H. Nakatsuka, *J. Opt. Soc. Am. B* **2**, 1634 (1985).
- ¹³R. Beach, D. DeBeer, and S. R. Hartmann, *Phys. Rev. A* **32**, 3467 (1985).
- ¹⁴M. A. Vasil'eva, J. Vischakas, V. Kabelka, and A. V. Masalov, *Opt. Commun.* **53**, 412 (1985).
- ¹⁵D. DeBeer, L. G. Van Wagenen, R. Beach, and S. R. Hartmann, *Phys. Rev. Lett.* **56**, 1128 (1986).
- ¹⁶M. Defour, J. C. Keller, and J. L. Le Gouët, *J. Opt. Soc. Am. B* **3**, 544 (1986).
- ¹⁷N. Morita, K. Torizuka, and T. Yajima, *J. Opt. Soc. Am. B* **3**, 548 (1986).
- ¹⁸J. E. Golub and T. W. Mossberg, *J. Opt. Soc. Am. B* **3**, 554 (1986).
- ¹⁹M. Tomita and M. Matsuoka, *J. Opt. Soc. Am. B* **3**, 560 (1986).
- ²⁰T. Hattori, A. Terasaki, and T. Kobayashi, *Phys. Rev. A* **35**, 715 (1987).
- ²¹T. Hattori and T. Kobayashi, *Chem. Phys. Lett.* **133**, 230 (1987).
- ²²R. W. Hellwarth, *Prog. Quantum Electron.* **5**, 1 (1977).
- ²³J. W. Goodman, *Statistical Optics* (Wiley, New York, 1985).
- ²⁴J. L. Oudar, *IEEE J. Quantum Electron.* **QE-19**, 713 (1983).
- ²⁵J. Etchepare, G. Grillon, I. Thomazeau, A. Migus, and A. Antonetti, *J. Opt. Soc. Am. B* **2**, 649 (1985).